Published in final edited form as:
Lasers Surg Med. 2010 January ; 42(1): 38. doi:10.1002/lsm.20887.

Photodynamic Therapy for Methicillin-Resistant *Staphylococcus aureus* Infection in a Mouse Skin Abrasion Model

Tianhong Dai, PhD[1,2], **George P. Tegos, PhD**[1,2], **Timur Zhiyentayev, MS**[1,3], **Eleftherios Mylonakis, MD, PhD**[4], and **Michael R. Hamblin, PhD**[1,2,5,*]

[1] Wellman Center for Photomedicine, Massachusetts General Hospital, Boston, Massachusetts 02114

[2] Department of Dermatology, Harvard Medical School, Boston, Massachusetts 02115

[3] Chemistry Department, Massachusetts Institute of Technology, Cambridge, Massachusetts 02139

[4] Department of Infectious Disease, Massachusetts General Hospital, Boston, Massachusetts 02114

[5] Harvard-MIT Division of Health Sciences and Technology, Cambridge, Massachusetts 02139

Abstract

Background and Objective—Methicillin-resistant *Staphylococcus aureus* (MRSA) skin infections are now known to be a common and important problem in the Unites States. The objective of this study was to investigate the efficacy of photodynamic therapy (PDT) for the treatment of MRSA infection in skin abrasion wounds using a mouse model.

Study Design/Materials and Methods—A mouse model of skin abrasion wound infected with MRSA was developed. Bioluminescent strain of MRSA, a derivative of ATCC 33591, was used to allow the real-time monitoring of the extent of infection in mouse wounds. PDT was performed with the combination of a polyethylenimine (PEI)–ce6 photosensitizer (PS) and non-coherent red light. In vivo fluorescence imaging was carried out to evaluate the effect of photobleaching of PS during PDT.

Results—In vivo fluorescence imaging of conjugate PEI–ce6 applied in mice indicated the photobleaching effect of the PS during PDT. PDT induced on average 2.7 $\log_{10}$ of inactivation of MRSA as judged by loss of bioluminescence in mouse skin abrasion wounds and accelerated the wound healing on average by 8.6 days in comparison to the untreated infected wounds. Photobleaching of PS in the wound was overcome by adding the PS solution in aliquots.

Conclusion—PDT may represent an alternative approach for the treatment of MRSA skin infections.

Keywords

photodynamic therapy; MRSA; wound infection; skin abrasion; mouse model; bioluminescence imaging; fluorescence imaging

*Correspondence to: Michael R. Hamblin, PhD, BAR414, Wellman Center for Photomedicine, Massachusetts General Hospital, 40 Blossom Street, Boston, MA 02114. hamblin@helix.mgh.harvard.edu.

INTRODUCTION

In the past decade there has been a dramatic increase in community-associated methicillin-resistant *Staphylococcus aureus* (CA-MRSA) infections [1,2]. Toxin-producing CA-MRSA strains are becoming the leading cause of skin infections presenting to emergency departments and out-patient settings in the United States [3]. The emergence of highly virulent CA-MRSA strains has been linked to the carriage of genes encoding Panton-Valentine leukocidin (PVL), a two-component leukolytic toxin [4,5]. Skin injuries susceptible to MRSA infections include cuts, abrasions, turf burns, etc. In some cases of MRSA skin infections, significant morbidity can occur, and in others infections can result in life threatening conditions [6,8].

Photodynamic therapy (PDT) was discovered over 100 years ago by observing the killing of microorganisms when harmless dyes and visible light were combined in vitro. Since then it has primarily been developed as a treatment for cancer, ophthalmologic disorders, and in dermatology. However in recent years interest in the antimicrobial effects of PDT has been revived, motivated by the rapidly increasing emergence of antibiotic resistance amongst pathogenic bacteria, and it has been proposed as a therapy for a large variety of localized infections [9,10]. PDT provides significant advantages over existing antimicrobial therapies. It appears equally effective to kill multi-drug resistance microbes as naïve strains, acts remarkably faster against microorganisms than antimicrobials, and furthermore there is no reported evidence for PDT resistant mechanisms.

In this report we describe the development of a mouse model of a skin abrasion wound infected with MRSA by using a bioluminescent MRSA strain derived from ATCC 33591. As the bacterial luminesence is linearly proportional to bacterial colony forming units (CFU) [11, 12], the bioluminescent bacteria allow the bioluminescence imaging of the course of the infection non-invasively in real-time. We used a highly effective antimicrobial photosensitizer (PS) composed of chlorin(e6) covalently linked to the basic polymer, polyethylenimine (PEI)–ce6. Topical application of PEI–ce6 to the infected abrasion was carried out followed by illumination after 5 minutes with red light.

MATERIALS AND METHODS

Bacterial Strain and Culture Conditions

The MRSA strain used was the stably bioluminescent MRSA Xen31 (Xenogen Corp., Alameda, CA), which was derived from the parental strain *S. aureus* ATCC 33591. The bioluminescent strain was transformed with a chromosomal copy of the modified *Photorhabdus luminescens* luxABCDE operon [13]. The bacteria were grown overnight in brain heart infusion (BHI) medium at 37°C with shaking at 100 rpm. Cell growth was assessed with an Evolution 300 UV–Vis Spectrophotometer (Thermo Scientific, Waltham, MA). When cultures reached an optical density (OD_{600}) of 0.8, which corresponds to a bacterial cell density of 10^8 CFU/ml, they were washed and resuspended in phosphate-buffered saline (PBS) (Dulbecco) at 2×10^9 CFU/ml.

Fluorescence Imaging for Detecting Photobleaching of Conjugate PEI–ce6

Prior to imaging, mice were anesthetized by intraperitoneal (i.p.) injections of a cocktail composed of 100 mg/kg ketamine and 10 mg/kg xylazine. A Maestro™ in vivo imaging system (CRI, Inc., Woburn, MA) was used to detect the fluorescence of conjugate PEI–ce6 applied to mice. Fluorescence images were taken with an excitation filter of 490 nm and an emission filter of 515 nm long pass. The correct exposure time was determined by the Maestro software (version 2.60). Detection was set to capture images at 10 nm increments from 500 to 720 nm.

The resulting images were loaded to the Maestro software and the fluorescence intensity was quantified.

Mouse Model of Skin Abrasion Infected MRSA

Adult female BALB/c mice (Charles River Laboratories, Wilmington, MA), 6–8 week old and weighing 17–21 g, were used. The animals were housed one per cage and maintained on a 12-hour light/dark cycle with access to food and water ad libitum. All animal procedures were approved by the Subcommittee on Research Animal Care (IACUC) of Massachusetts General Hospital and met the guidelines of National Institutes of Health (NIH). At days 4 and 1 before the infection, mice were administered two doses of cyclophosphamide. The first dose, 150 mg cyclophosphamide per kg mouse body weight (150 mg/kg) was injected i.p. followed by the second dose of 100 mg/kg. This treatment reduced peripheral blood neutrophils to <100/μl blood, fostering a more vulnerable environment in the mice to infection.

Before the creation of wounds, mice were anesthetized with i.p. injections of ketamine/xylazine cocktail and then shaved on the dorsal surfaces. Skin abrasion wounds were made on the dorsal surfaces of mice using 28-gauge needles (Micro-Fine IV, Becton Dickinson, Franklin Lakes, NJ) by creating 6×6 crossed scratch lines within a defined 1×1 cm^2 area (Fig. 1). The scratches were made in such a manner that they only damaged the stratum corneum and upper-layer of the epidermis but not the dermis. Five minutes after wounding, an aliquot of 50 μl suspension containing 10^8 CFU of bioluminescent MRSA in PBS was inoculated over each defined area containing the crossed scratches with a pipette tip. Bioluminescence images were taken immediately after the inoculation of bacteria and on a daily basis thereafter.

Preparation of PEI–ce6 Conjugate

PEI–ce6 conjugate was prepared by a modification of the method described previously [14]. In brief, cross-linked PEI (high molecular weight 10,000–25,000, Aldrich catalog number 40,872-7) was reacted with ce6 (Frontier Scientific, Logan, UT) and 1-ethyl-3-(3-dimethylaminopropyl)-carbodiimide hydrochloride (Sigma-Aldrich Co., St. Louis, MO) in borate buffer (0.1 M, pH = 8.5), for 24 hours in the dark. The crude conjugate was purified by precipitation from acetone at −20°C followed by exhaustive (2 days, three changes) dialysis (MW cutoff 2 kDa) against distilled water containing 0.1% Triton X-100 The substitution ratio was calculated, from the absorption spectrum of the conjugate (0.1 M NaOH, 1% SDS), to be an average of 1 ce6/PEI-chain, assuming that the absorption coefficient of conjugated ce6 was the same as that of free ce6 ($\varepsilon_{400\,nm}$ = 150,000 M^{-1} cm^{-1}) and the trinitrobenzene sulfonic acid assay for free amino groups [15].

Bioluminescence Imaging

An ICCD photon-counting camera (Model C2400-30H; Hamamatsu Photonics, Bridgewater, NJ) was used. The camera was mounted in a light-tight specimen chamber, fitted with a light-emitting diode, a set-up that allowed for a background gray-scale image of the entire mouse to be captured. By accumulating many images containing binary photon information (an integration time of 2 minutes was used), a pseudo-color luminescence image was generated. Superimposition of this image onto the gray-scale background image yielded information on the location and intensity in terms of photon number. The camera was also connected to a computer system with Microsoft Windows 98 through an image processor (Argus-50, Hamamatsu Photonics). Argus-50 control program (Hamamatsu Photonics) was used to acquire images and to process the image data collected.

Prior to imaging, mice were anesthetized by i.p. injections of ketamine/xylazine cocktail. Mice were then placed on an adjustable stage in the specimen chamber, and the wounds were positioned directly under the camera. A gray-scale background image of each wound was made,

and this was followed by a photon count of the same region. This entire wound photon count was quantified as relative luminescence units (RLUs) and was displayed in a false color scale ranging from pink (most intense) to blue (least intense).

Photodynamic Therapy for MRSA Infection in Mouse Skin Abrasions

PS was added at 30 minutes after infection, allowing the bacteria to bind the host tissue. To take the effect of photobleaching into account, conjugate PEI–ce6 was added as aliquots of 20, 10, 10, 10, and 10 μl of a solution in PBS (400 μM ce6 equivalent) at the time points when the light doses of 0, 84, 180, 240, and 300 J/cm^2 had been delivered, respectively. Five minutes after the first addition to allow the conjugate to bind and penetrate the bacteria the mice were again imaged to quantify any dark toxicity of the conjugate to the bacteria.

Mice were illuminated with 660 ± 15 nm light delivered in a spot with diameter 2.5-cm that covered the abrasion from a non-coherent light source (LumaCare, Newport Beach, CA). The irradiance was routinely measured using a LaserMate™ power meter (Coherent, Portland, OR), and irradiance used was 100 mW/cm^2. Mice were given total light doses of up to 360 J/cm^2 in aliquots with bioluminescence imaging taking place after each aliquot of light.

Statistics

In the two-dimensional coordinates system, areas under the curves (AUC) representing the time courses of bacterial luminescence of wounds were calculated using numerical integration [16]. Differences in the AUC between control and treated mice were compared for statistical significance using a *t*-test for two samples assuming unequal variance. Wound healing analysis was performed using Kaplan–Meier method. The wound healing rates were tested for significance by the use of a log-rank test [17]. The values of $P<0.05$ were considered statistically significant.

RESULTS

Photobleaching of Conjugate PEI–ce6 During PDT

The successive fluorescence images of a mouse treated with a single PEI–ce6 aliquot and a mouse with multiple PEI–ce6 aliquots are presented in Figure 2A,B, respectively. For the mouse given a single PEI–ce6 aliquot (50 μl), the aliquot was applied onto the back of the mouse at the beginning of PDT; for the one applied with multiple PEI–ce6 aliquots, the PS was applied as 20, 10, 10, and 10 μl solution when 0, 4, 8, and 12 J/cm^2 light had been delivered. In the mouse with a single PEI–ce6 aliquot, fluorescence loss was observed in a light dose-dependent manner, indicating the photobleaching of PEI–ce6 during PDT (Fig. 2A). The remaining fractions of fluorescence were 100%, 67%, 36%, 19%, and 13% when 0, 4, 8, 12, and 16 J/cm^2 light had been delivered (Fig. 2C). For the mouse applied with multiple aliquots of PEI–ce6, the fluorescence was brought back to approximately the initial intensity by adding 10 μl PEI–ce6 solution at the time points when 4, 8, and 12 J/cm^2 light had been delivered. The remaining fraction of fluorescence in this mouse was 73% when 16 J/cm^2 light had been delivered (Fig. 2C).

MRSA Infection in Mouse Skin Abrasion Wound

By applying 10^8 CFU of MRSA topically onto skin abrasion wounds made on the shaved backs of adult female BALB/c mice, a stable infection was developed in the mouse wounds as characterized by bioluminescence imaging. Figure 3A shows the successive bacterial luminescence images of a representative mouse skin abrasion wound infected with MRSA. After infection, the bacterial luminescence remained strong and stable until day 5 and detectable until day 12. Gram-staining of the histological section of a representative skin

abrasion specimen (harvested at day 3 post-infection) (Fig. 3B) showed that MRSA was localized superficially in the epidermis.

PDT Responses of MRSA in Mouse Skin Abrasion Wounds

Figure 4A shows the PDT dose–response of bacterial luminescence of a representative mouse skin abrasion wound infected with MRSA and treated with PDT as well as a mouse skin abrasion wound infected with MRSA and treated with PEI–ce6 only (dark control), respectively. PDT gave a light dose-dependent reduction of bacterial luminescence from the mouse wound until over 99% was gone at 240 J/cm^2, while during the same period of time the bacterial luminescence was largely preserved in the dark control.

Figure 4B shows the average (± SD) reduction in bacterial luminescence from 10 mice each of which was treated with PDT. After 360 J/cm^2 light was delivered, PDT on average gave 2.7-log$_{10}$ of reduction of bacterial luminescence in a light dose dependent manner.

The time courses of the mean bacterial luminescence of the infected mouse wounds treated with PDT (n = 10) and without treatment (n = 12) are shown in Figure 4C. Some bacterial re-growth in the PDT-treated wounds was observed but was generally modest. The averaged bacterial luminescence intensity of the PDT-treated wounds after re-growth was on average 1.3-log$_{10}$ lower than that of the non-treated wounds at the same time points. Statistical comparison of AUC in Figure 4C showed that PDT significantly decreased bacterial bio-burden of the infected wounds (P<0.0001) (Fig. 4D).

Wound Healing

Figure 5A shows the Kaplan–Meier wound healing curves of the non-treated mice (n = 12) and the mice treated with PDT (n = 10). Statistical analysis indicated that PDT-treated mice had a significant advantage in wound healing over the non-treated mice. The average wound healing times of the PDT-treated mice and non-treated ones were 5.6 ± 5.1 and 14.2 ± 2.6 days (P = 0.0002), respectively. In 60% (6 out of 10) of the PDT-treated mice, complete wound healing was achieved within 4 days post-infection. Three PDT-treated mice had relative longer wound healing times from days 11 to 15 post-infection. In these mice, moderate reoccurrence of infection after PDT was observed. Figure 5B,C representatively shows the wound morphologies at day 4 post-infection of a mouse treated with PDT and one without treatment. In the PDT-treated wound, no visible scratch was observed (Fig. 5B) and no bacterial luminescence was detected; while in the non-treated wound, the scratches were expanded (Fig. 5C) and infections were spread over the area surrounding the scratches as indicated by bioluminescence imaging (RLUs = 7.45×10^5).

Body Weight

Figure 6 compares the mean body weights of the PDT-treated mice (n = 10) and non-treated mice (n = 12) over 4 days post-infection when the most severe morbidities occurred. In the non-treated mice, a more rapid weight loss pattern was observed than in the PDT treated ones. At day 2 post-infection when the maximum weight loss occurred, the weight loss of the non-treated mice was 11.6 ± 4.0% of the initial weight, while the weight loss of the PDT-treated mice was only 6.1 ± 3.4% (P = 0.0009).

DISCUSSION

In the United States, MRSA is a major cause of skin infections [3]. Recently, highly virulent strains of MRSA have caused outbreaks of serious infections among individuals in close contact, particularly where skin trauma is likely, including sports teams, military recruits,

infection drug users, prisoners, and others. Infections due to MRSA can manifest as severe boils and other skin infections, infections in joints, pneumonia, and even death.

In this study, we present a new mouse model of a skin abrasion wound infected with MRSA to mimic the same disease in humans. To be of potential clinical value, a valid animal model must resemble this host-pathogen interaction as close as possible to human infected wounds. In the present mouse model, the superficial scratches were made on the shaved backs of mice followed by the topical application of MRSA suspension. A stable and reproducible chronic wound infection was observed in mice as demonstrated by bioluminescence imaging. Biofilms of MRSA were observed within the wounds, representing a typical situation of chronic and persistent infection [18]. The infections, when without intervention, caused severe morbidity in mice as indicated by loss of body weight. In addition, the use of bioluminescent bacteria allowed the real-time monitoring of the extent of infection in mouse wounds. This method is an improvement on the traditional use of survival or body fluid sampling and subsequent plating and colony counting. The first method suffers from the disadvantage of being wasteful of animals, and does not apply when the bacteria are non-invasive such as MRSA, while the second method suffers from the disadvantage that tissue sampling introduces another source of experimental error, is laborious and does not give real-time results. To the best of the authors' knowledge, the present study is the first report on the mouse model of skin abrasion wound infected with a bioluminescent MRSA strain.

We investigated the efficacy of PDT in vivo for treating MRSA infection in skin abrasion wounds, with the combination of PEI–ce6 conjugate and red light. Findings from this study demonstrated that PDT significantly reduced the bio-burden of MRSA in the mouse wounds, which would otherwise develop severe infections. In addition, wound healing and morbidity (body weight loss) were greatly benefited by the eradication of MRSA from the wounds. The rapid wound healing in the PDT-treated mice was due to the fact that the scratches were surrounded by non-wounded healthy tissue, and thus, the migration path of keratinocytes was short once the bacteria that prevented healing had been eliminated. We believe that this phenomenon of rapid wound healing is similar to the rapid healing observed after fractional laser treatment of the skin [19]. In contrast, in the non-treated mice, the infection spread out from the scratches to the surrounding non-wounded tissue, and subsequently damaged the healthy tissue, resulting in a marked delay in wound healing. It has been demonstrated that the disruption of wound healing by *S. aureus* is specially dependant on the ability of this organism to form bio-films, which inhibit reepithelialization [20].

It is commonly observed that fewer $\log_{10}$ of PDT inactivation of bacteria can be achieved in vivo than in vitro (in vitro inactivation of bacteria using PDT can reach up to 5–6 $\log_{10}$, data not shown). There are two factors that are responsible for this. First, the host tissue competes with the bacteria for binding the PS, resulting in a reduced efficacy of in vivo bacterial inactivation where the bacteria are embedded in tissue. Second, bacteria tend to penetrate into the tissue over the time and form biofilms in the deep sites. Biofilms behave as a barrier for the PS to access the bacteria inside the biofilm. Additionally, the concentration of the PS, which are applied topically, will decrease in the deep site of tissue, and the light dose will also attenuate exponentially while light penetrates into the tissue.

It is well known that PS can be degraded or modified by light during PDT [21]. This phenomenon is called photobleaching and can be observed by the loss of fluorescence of PS in tissue, cells, or solutions during light exposure. Photobleaching is the light-dependent chemical destruction of a PS molecule that results in loss of the chromophore, and corresponding loss of ability to absorb light in the visible spectral region [22]. Photobleaching of PS may result in a reduced yield of inactivation of bacteria per incident photon. Conjugate PEI–ce6 was used as the PS in the study. It was found that photobleaching of conjugate PEI–

ce6 occurred during PDT. As a result, to ensure a sufficient effect of PDT, one needs to apply PS in multiple aliquots to counteract the effect of photobleaching on PS.

On the other hand, it has been proposed that photobleaching may be used to increase the therapeutic ratio of PDT in the clinical situation [21]. As the cationic PEI–ce6 selectively binds bacteria over host tissue, the concentration of PS within host tissue is lower than that in bacteria. It may be possible to apply PS at a low dose, so that it is photodegraded before it is able to cause any large photodynamic damage to normal tissue. The bacteria, however, in which the concentration of PS is higher, may be completely photoinactivated. Therefore, photobleaching may influence the therapeutic ratio positively or negatively and should be carefully considered in the application of PDT.

In conclusion, based on the findings in the present study, PDT may represent an alternative approach for the treatment of MRSA infections in sports and other skin wounds. Future clinical studies are warranted.

Acknowledgments

This work was supported by the NIH (grant AI050875 to M.R.H.) and DOD/AFOSR FA9550-04-1-0079. T.D. was supported by a Bullock-Wellman Fellowship Award and GPT by a Massachusetts Technology Transfer Center Award. T.D. also received a travel grant from the ASLMS for attending the 29th ASLMS Annual Conference and presenting the preliminary data. This contribution satisfies the condition of the travel grant that a manuscript should be submitted to the LSM within 1 year after the annual conference. We are grateful to Christopher H. Contag, Tayyaba Hasan, and Albert T. McManus for helpful advice and discussion and to Xenogen Corp. (now Caliper Life Sciences) for the gift of XEN31.

Contract grant sponsor: NIH; Contract grant number: AI050875; Contract grant sponsor: DOD/AFOSR; Contract grant number: FA9550-04-1-0079.

References

1. Herold BC, Immergluck LC, Maranan MC, Lauderdale DS, Gaskin RE, Boyle-Vavra S, Leitch CD, Daum RS. Community-acquired methicillin-resistant *Staphylococcus aureus* in children with no identified predisposing risk. JAMA 2008;279:593–598. [PubMed: 9486753]
2. Chambers HF. The changing epidemiology of *Staphylococcus aureus*? Emerg Infect Dis 2001;7:178–182. [PubMed: 11294701]
3. Zervos M. Treatment options for uncomplicated community-acquired skin and soft tissue infections caused by methicillin-resistant Staphylococcus aureus: Oral antimicrobial agents. Surg Infect (Larchmt) 2008;9:s29–s34. [PubMed: 18844472]
4. Vandenesch F, Naimi T, Enright MC, Lina G, Nimmo GR. Community-acquired methicillin-resistant Staphylococcus aureus carrying Panton-Valentine leukocidin genes: Worldwide emergence. Emerg Infect Dis 2003;9:978–984. [PubMed: 12967497]
5. Diep BA, Otto M. The role of virulence determinants in community-associated MRSA pathogenesis. Trends Microbiol 2008;16:361–369. [PubMed: 18585915]
6. Bowers AL, Huffman GR, Sennett BJ. Methicillin-resistant Staphylococcus aureus infections in collegiate football players. Med Sci Sports Exerc 2008;40:1362–1367. [PubMed: 18614960]
7. Philadelphia High School Football Player Dies of MRSA Infection. [Accessed September 2009]. http://cherryhill.injur-yboard.com/
8. Turbeville SD, Cowan LD, Greenfield RA. Infectious disease outbreaks in competitive sports: A review of the literature. Am J Sports Med 2006;34:1860–1865. [PubMed: 16567462]
9. Hamblin MR, Hasan T. Photodynamic therapy: A new antimicrobial approach to infectious disease? Photochem Photobiol Sci 2004;3:436–450. [PubMed: 15122361]
10. Jori G. Photodynamic therapy of microbial infections: State of the art and perspectives. J Environ Pathol Toxicol Oncol 2006;25:505–519. [PubMed: 16566738]

11. Demidova TN, Gad F, Zahra T, Francis KP, Hamblin MR. Monitoring photodynamic therapy of localized infections by bioluminescence imaging of genetically engineered bacteria. J Photochem Photobiol B 2005;81:15–25. [PubMed: 16040251]
12. Thorn RM, Nelson SM, Greenman J. Use of a bioluminescent Pseudomonas aeruginosa strain within an in vitro micro-biological system, as a model of wound infection, to assess the antimicrobial efficacy of wound dressings by monitoring light production. Antimicrob Agents Chemother 2007;51:3217–3224. [PubMed: 17638701]
13. Francis KP, Yu J, Bellinger-Kawahara C, Joh D, Hawkinson MJ, Xiao G, Purchio TF, Caparon MG, Lipsitch M, Contag PR. Visualizing pneumococcal infections in the lungs of live mice using bioluminescent Streptococcus pneumoniae transformed with a novel gram-positive lux transposon. Infect Immun 2001;69:3350–3358. [PubMed: 11292758]
14. Tegos GP, Anbe M, Yang C, Demidova TN, Satti M, Mroz P, Janjua S, Gad F, Hamblin MR. Protease-stable polycationic photosensitizer conjugates between polyethyleneimine and chlorin(e6) for broad-spectrum antimicrobial photoinactivation. Antimicrob Agents Chemother 2006;50:1402–1410. [PubMed: 16569858]
15. Habeeb AF. Determination of free amino groups in proteins by trinitrobenzenesulfonic acid. Anal Biochem 1966;14:328–336. [PubMed: 4161471]
16. Davis, PJ.; Rabinowitz, P. Methods of numerical integration. New York: Academic Press; 1975. p. 459
17. Peto R, Peto J. Asymptotically efficient rank invariant test procedures. J Royal Stat Soc A 1972;135:185–207.
18. James GA, Swogger E, Wolcott R, Pulcini E, Secor P, Sestrich J, Costerton JW, Stewart PS. Biofilms in chronic wounds. Wound Repair Regen 2008;16:37–44. [PubMed: 18086294]
19. Manstein D, Herron GS, Sink RK, Tanner H, Anderson RR. Fractional photothermolysis: A new concept for cutaneous remodeling using microscopic patterns of thermal injury. Lasers Surg Med 2004;34:426–438. [PubMed: 15216537]
20. Schierle CF, De la Garza M, Mustoe TA, Galiano RD. Staphylococcal biofilms impair wound healing by delaying reepithelialization in a murine cutaneous wound model. Wound Repair Regen 2009;17:354–359. [PubMed: 19660043]
21. Ma LW, Moan J, Berg K. Comparison of the photobleaching effect of three photosensitizing agents: Meso-tetra(m-hydroxyphenyl)chlorin, meso-tetra(m-hydroxyphenyl)por-phyrin and photofrin during photodynamic therapy. Lasers Med Sci 1994;9:127–132.
22. Plaetzer K, Krammer B, Berlanda J, Berr F, Kiesslich T. Photophysics and photochemistry of photodynamic therapy: Fundamental aspects. Lasers Med Sci 2009;24:259–268. [PubMed: 18247081]

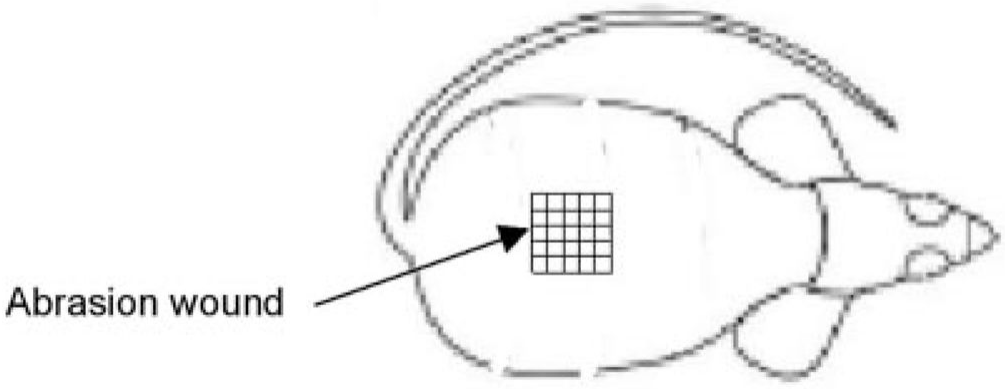

Fig. 1.
Mouse model of skin abrasion.

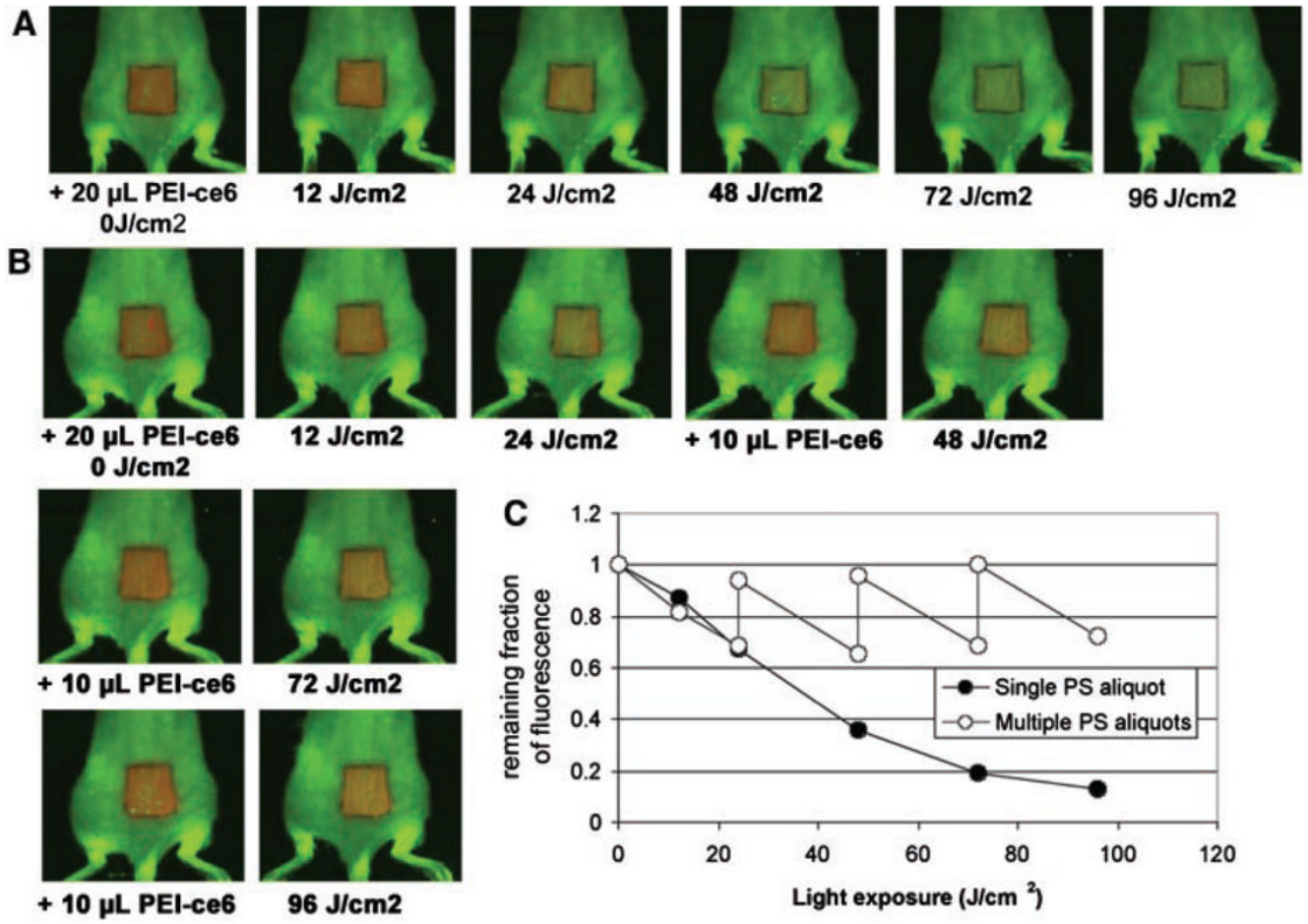

Fig. 2.

A: Successive fluorescence images of conjugate PEI–ce6 in a mouse given a single 20 µl aliquot on the back during PDT. **B**: Successive fluorescence images of conjugate PEI–ce6 applied in a mouse with multiple aliquots of 20, 10, 10, and 10 µl at the time points when 0, 24, 48, 72 J/cm^2 light had been delivered during PDT. **C**: Remaining fractions of fluorescence of conjugate PEI–ce6 in the mice noted in A and B.

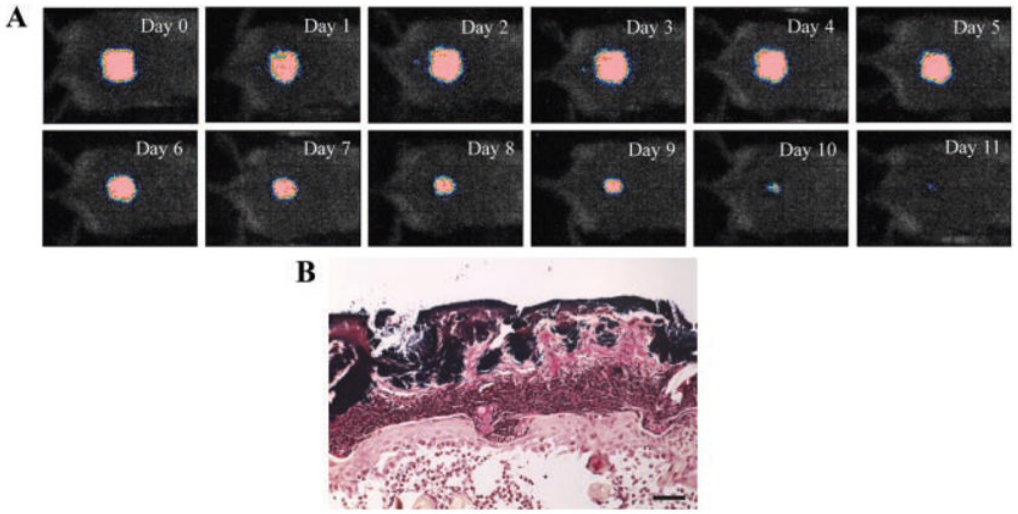

Fig. 3.

A: Successive bioluminescence images of a representative mouse skin abrasion wound infected with luminescent MRSA. **B**: A Gram-stained section of a mouse skin abrasion specimen showing the bio-films formed by Gram-positive MRSA near the skin surface. Dark blue area: bio-films of MRSA. The mouse skin abrasion specimen was harvested at day 3 post-infection.

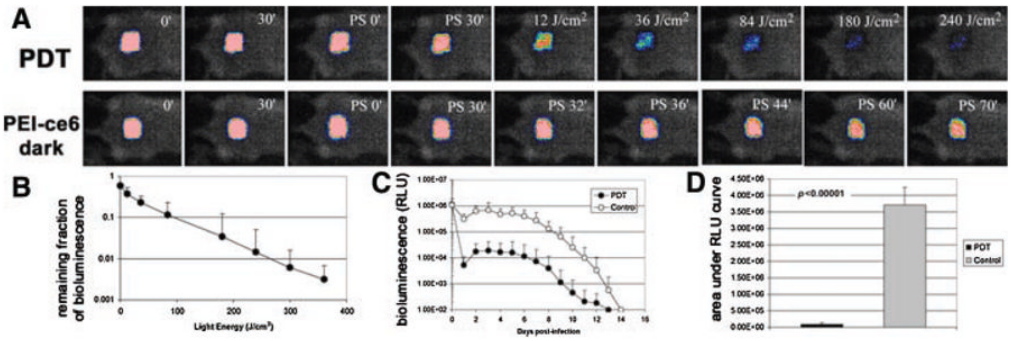

Fig. 4.

A: Dose–response of bacterial luminescence of a mouse abrasion wound infected with MRSA and treated with PDT; and dose–response of bacterial luminescence of a mouse abrasion wound infected with MRSA and treated with conjugate PEI–ce6 only. PDT was carried out at 30 minutes after infection. **B**: Dose–response of mean bacterial luminescence of the mouse wounds infected with MRSA and treated with PDT ($n = 10$). **C**: Time courses of bacterial luminescence of the infected abrasion wounds in the PDT-treated mice ($n = 10$) and non-treated mice ($n = 12$). **D**: Mean areas under the bioluminescence versus time plots (in the two-dimensional coordinate system in (C), representing the overall bacterial burden of mouse abrasion wounds in different groups. Bars: standard deviation.

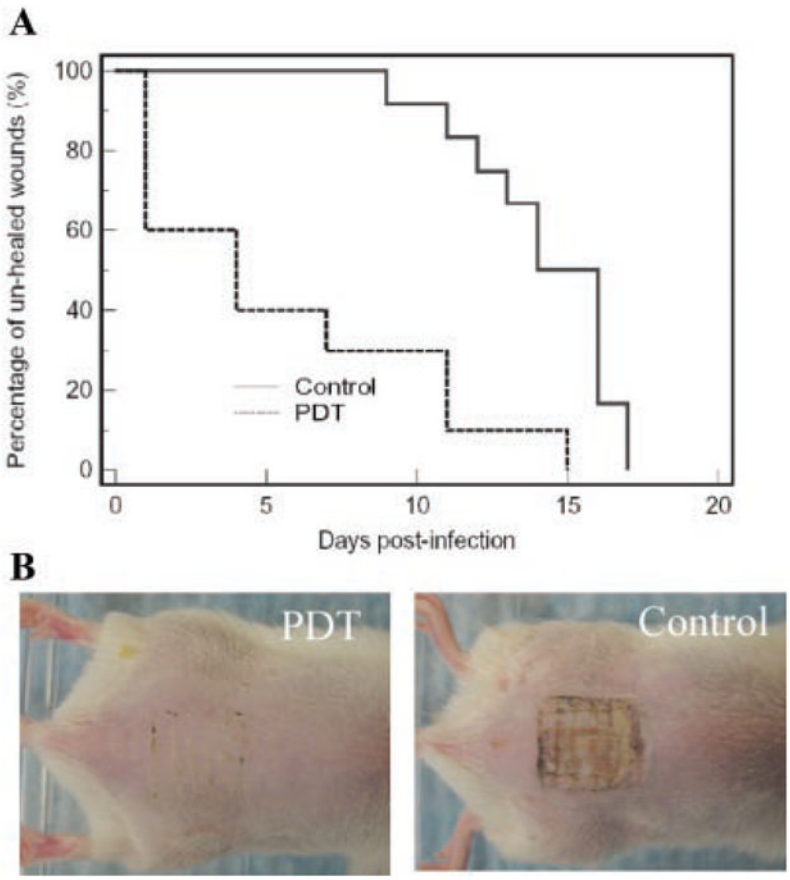

Fig. 5.

A: Kaplan–Meier wound healing curves of MRSA infected mouse abrasion wounds without treatment (neither PS nor light was applied) and treated with PDT, respectively. **B**: Wound morphologies at day 4 post-infection of a representative PDT-treated mouse wound and a non-treated mouse wound.

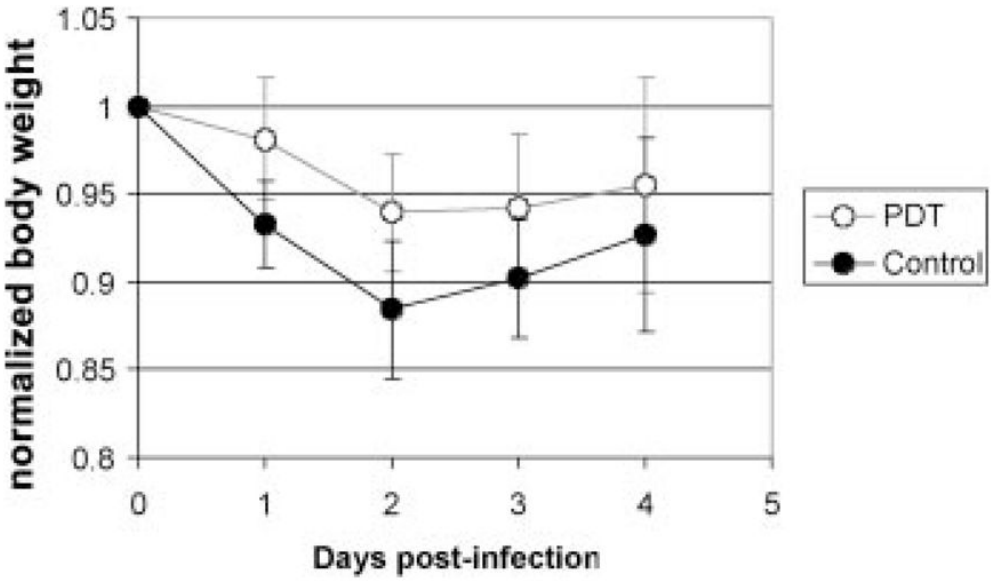

Fig. 6.

Time courses of the mean normalized body weight of PDT-treated mice and non-treated mice over 4 days post-infection. Bars: standard deviation.